Effects of polymorphism on the microenvironment of the LDL receptor-binding region of human apoE

Sissel Lund-Katz,[1,*] Suzanne Wehrli,[*] Mohamed Zaiou,[†] Yvonne Newhouse,[§] Karl H. Weisgraber,[§,,††] and Michael C. Phillips[*]**

Joseph Stokes, Jr. Research Institute,* ARC, Suite 302, Children's Hospital of Philadelphia, University of Pennsylvania School of Medicine, Philadelphia, PA 19104; Department of Biochemistry,† MCP Hahnemann University, Philadelphia, PA 19129; and Gladstone Institute of Cardiovascular Disease,§ Cardiovascular Research Institute,** and Department of Pathology,†† University of California, San Francisco, San Francisco, CA 94110

Abstract **To understand the molecular basis for the differences in receptor-binding activity of the three common human apolipoprotein E (apoE) isoforms, we characterized the microenvironments of their LDL receptor (LDLR)-binding regions (residues 136–150). When present in dimyristoyl phosphatidylcholine (DMPC) complexes, the 22-kDa amino-terminal fragments (residues 1–191) of apoE3 and apoE4 bound to the LDLR with ~100-fold greater affinity than the 22-kDa fragment of apoE2. The pK_a values of lysines (K) at positions 143 and 146 in the LDLR-binding region in DMPC-associated 22-kDa apoE fragments were 9.4 and 9.9 in apoE2, 9.5 and 9.2 in apoE3, and 9.9 and 9.4 in apoE4, respectively. The increased pK_a of K146 in apoE2 relative to apoE3 arises from a reduction in the positive electrostatic potential in its microenvironment. This effect occurs because C158 in apoE2, unlike R158 in apoE3, rearranges the intrahelical salt bridges along the polar face of the amphipathic α-helix spanning the LDLR-binding region, reducing the effect of the R150 positive charge on K146 and concomitantly decreasing LDLR-binding affinity. The C112R mutation in apoE4 that differentiates it from apoE3 did not perturb the pK_a of K146 significantly, but it increased the pK_a of K143 in apoE4 by 0.4 pH unit. This change did not alter LDLR-binding affinity. Therefore, maintaining the appropriate positive charge at the C-terminal end of the receptor-binding region is particularly critical for effective interaction with acidic residues on the LDLR.**—Lund-Katz, S., S. Wehrli, M. Zaiou, Y. Newhouse, K. H. Weisgraber, and M. C. Phillips. **Effects of polymorphism on the microenvironment of the LDL receptor-binding region of human apoE.** ***J. Lipid Res.*** **2001.** 42: **894–901.**

Supplementary key words apolipoprotein E2 • apolipoprotein E3 • apolipoprotein E4 • lysine pK_a • amphipathic α-helix • receptor-binding affinity

Apolipoprotein E (apoE), a constituent of several plasma lipoproteins, mediates the catabolism of lipoprotein particles by binding to receptors of the LDL receptor (LDLR) family and to cell surface heparan sulfate proteoglycans (1). It also participates in the lipolytic conversion of VLDL and its intermediates and promotes VLDL triglyceride production (2). ApoE contains two structural domains that also define functional domains: the amino-terminal domain (residues 1–191) contains the LDLR-binding region (vicinity of residues 136–150), and the carboxyl-terminal domain (residues 218–299) contains the major lipoprotein-binding elements (3).

Human apoE is a polymorphic protein with three common isoforms. ApoE3, the most common, has cysteine at position 112 (C112) and arginine at position 158 (R158), whereas apoE2 has cysteine at both positions and apoE4 has arginine (3). These differences have profound functional consequences. ApoE2 binds defectively to the LDLR (4) and is associated with type III hyperlipoproteinemia, a disorder characterized by the accumulation of chylomicron remnants in plasma and increased atherosclerosis (5). ApoE4 binds to the LDLR with the same affinity as apoE3 (4) but is associated with high plasma concentrations of cholesterol and LDL and increased risk of coronary heart disease (6–8); these effects are thought to reflect the preferential binding of apoE4 for VLDL. In contrast, apoE3 binds preferentially to HDL (3, 9). ApoE4 is also a major risk factor for Alzheimer's disease and poor outcome from stroke and head trauma (10).

The LDLR-binding region of apoE is highly enriched in basic amino acids (11). The positive electrostatic potential created by these residues gives rise to electrostatic attractions to acidic residues on the LDLR. Subtle changes within the receptor-binding region of apoE lead to defective receptor activity. For example, C158 in apoE2 causes defective binding to the LDLR although this residue lies outside the receptor-binding region. The primary cause for the defective binding is that the R158–D154 salt bridge in

Abbreviations: apo, apolipoprotein; δ, chemical shift; DMPC, dimyristoyl phosphatidylcholine; HSQC-NMR, heteronuclear single quantum coherence-nuclear magnetic resonance; LDLR, LDL receptor.

[1] To whom correspondence should be addressed.

apoE3 is replaced by an R150–D154 bridge in apoE2, which pulls R150 out of the LDLR-binding region, effectively reducing the positive electrostatic potential (12). In addition, the C-terminal domain in apoE2 interacts with the N-terminal domain, which further decreases receptor-binding activity (13).

Our understanding of the molecular basis for the functional differences in the apoE isoforms is largely based on analyses of their 22-kDa amino-terminal domains in the lipid-free state by X-ray crystallography. In all three isoforms, this domain consists of a four-helix bundle of elongated amphipathic α helices (12, 14–16). However, apoE in the lipid-free state is not recognized by the receptor (17). Only when apoE interacts with a phospholipid does the four-helix bundle open and adopt a receptor-active conformation (17–19).

To investigate the enhanced binding affinity to the LDLR induced by interaction of apoE with phospholipid, we used NMR to study the microenvironments of the eight lysines (K) in the 22-kDa fragment of apoE3 in the lipid-free and lipid-associated states (20). When the protein was complexed with dimyristoyl phosphatidylcholine (DMPC), K143 and K146 (both in the LDLR-binding region) had unusually low pK_a values (9.5 and 9.2, respectively), reflecting local increases in positive electrostatic potential caused by reorganization of the helices on lipid association. The increased electrostatic potential, coupled with enhanced exposure to the aqueous phase of the polar face of the amphipathic α-helix containing residues 136–150, seems to explain why lipid association is required for high affinity binding of apoE to the LDLR.

In the present study, we characterized the microenvironments of lysines in LDLR-binding regions of apoE2 and apoE4. The goal of the study was to gain additional insight into the structural basis of differences between the apoE3 and apoE4 domains, which bind normally to receptors, and the apoE2 domain, which does not.

EXPERIMENTAL METHODS

Materials

DMPC was purchased from Avanti Polar Lipids (Pelham, AL), and stock solutions were stored in chloroform–methanol 2:1 (v/v) under nitrogen at −20°C; the purity was assayed by TLC on silica gel G plates (Analtech, Newark, DE) in chloroform–methanol–water 65:25:4 (v/v/v). Lipids were visualized by spraying developed TLC plates with a 50% sulfuric acid solution and charring them at 200°C for 15 min; 100-μg quantities gave a single spot. 2-Mercaptoethylamine (cysteamine) was purchased from Sigma (St. Louis, MO). D_2O (Cambridge Isotope Laboratories, Andover, MA) was routinely deoxygenated and stored under nitrogen. [^{13}C]formaldehyde (99% isotopic enrichment) as a 20% solution in water and [ε-^{13}C]lysine dihydrochloride (6-^{13}C, 99%) were from Cambridge Isotope Laboratories. [^{14}C]Formaldehyde (55 Ci/mol) in distilled water was purchased from NEN Life Sciences (Boston, MA). Anionic contaminants were removed from the formaldehyde by passage through a small Dowex 1-chloride column (21). $NaCNBH_3$ (Aldrich, Milwaukee, WI) was recrystallized from methylene chloride before use (21). $K_3Fe(CN)_6$ was from Aldrich; other salts and reagents were analytical grade.

Bacteriological media were obtained from Difco Laboratories (Detroit, MI). The prokaryotic expression vector pET32a and the competent *Escherichia coli* strain BL21 (DE3) were from Novagen (Madison, WI). Competent *E. coli* strain DH5α and nucleotides were from Life Technologies (Gaithersburg, MD). *Pfu* DNA polymerase was from Stratagene (La Jolla, CA). Restriction enzymes were purchased from New England BioLabs (Beverly, MA). Isopropyl β-D-galactopyranoside, 2-mercaptoethanol, aprotinin, and ampicillin were from Sigma. Ultrapure guanidine hydrochloride was from ICN Pharmaceuticals (Costa Mesa, CA). Oligonucleotides were from Oligos Etc. (Wilsonville, OR), and DNA purification kits were from Qiagen (Chatsworth, CA).

Expression and purification of 22-kDa fragments and preparation of 22-kDa apoE·DMPC complexes

The 22-kDa fragments of apoE2, apoE3, and apoE4 were expressed in *E. coli* and purified as described (22). If further purification (>95%) was needed, the fragments were subjected to gel filtration with a Superdex 75 column.

To obtain 22-kDa apoE3 fragments enriched in [ε-^{13}C]lysine, the fragment was expressed and purified as described for selenomethionine labeling of apoE (23). Briefly, starter culture (1 ml) was added to 1,000 ml of lysine-free LeMaster medium (24) supplemented with 250 μl of Kao-Mychayluk vitamin solution (25) and 417 mg of [ε-^{13}C]lysine. Cultures were grown at 37°C to an optical density (at 600 nm) of 0.6 (8 h), induced with 0.5 mM isopropyl-β-D-thiogalactopyranoside, and harvested after 2 h. Incorporation of [ε-^{13}C]lysine was confirmed by electrospray mass spectrometry, performed by the Mass Spectrometry Facility at the University of California, San Francisco (San Francisco, CA). A molecular mass increase of 24 mass units indicated 50% incorporation of [ε-^{13}C]lysine into the eight lysine positions in the apoE3 22-kDa fragment.

The 22-kDa fragments of all three isoforms were complexed with DMPC and isolated by gel-filtration chromatography as described (20). The 22-kDa apoE·DMPC complexes were labeled with ^{13}C as described (26).

Cysteamine modification of 22-kDa apoE·DMPC complexes

The 22-kDa apoE2 fragment was modified with cysteamine as described (27). After reductive methylation, the 22-kDa apoE2·DMPC complexes were further modified by incubating 5 mg of 22-kDa apoE2 in 100 mM NH_4HCO_3 with 10 μl of cysteamine (100 mg/ml) per 150 μg of protein for 4 h at 37°C. The modified complexes were dialyzed against saline-EDTA followed by D_2O-borate buffer before use in NMR experiments.

NMR measurements

^{1}H-^{13}C heteronuclear single quantum coherence (HSQC) two-dimensional NMR spectra of ^{13}C-labeled 22-kDa apoE·DMPC complexes were obtained with a Bruker DMX400 wide-bore spectrometer equipped with an SGI 02 computer and a 5-mm inverse broad-band probe as previously described (20). The sample temperature for the two-dimensional NMR spectra was set at 310 K. The two-dimensional ^{1}H-^{13}C HSQC spectra were recorded with carbon decoupling during acquisition. The time-proportional phase-increment method (28) was used to obtain phase-sensitive spectra. One-dimensional ^{13}C spectra were obtained with proton composite pulse decoupling. Chemical shifts and line widths for lipid-protein complexes were measured as described elsewhere (20, 26, 29). The pseudocontact shifts observed when $K_3Fe(CN)_6$ was added to the aqueous phase were used to explore the exposure of [^{13}C]dimethyl lysines to the aqueous medium (29). The chemical shifts of [ε-^{13}C]dimethyl lysine and [ε-^{13}C]dimethyl-terminal amino residues of the com-

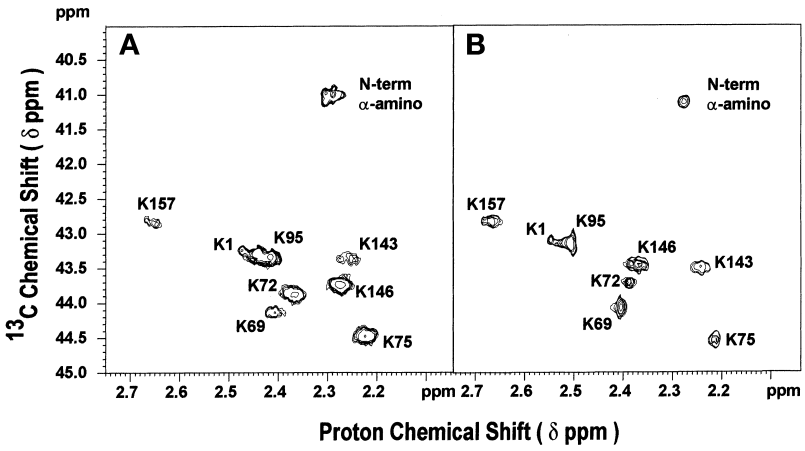

Fig. 1. Phase-sensitive ^{1}H, ^{13}C HSQC spectra of 22-kDa apoE·DMPC (1:3.2, w/w) discoidal complexes showing [^{13}C]dimethyl lysine resonances. The spectra were obtained under conditions similar to those described previously (20). Sequence-specific assignments for (A) 22-kDa apoE3·DMPC (pH 10.0) (20) and (B) 22-kDa apoE2·DMPC (pH 10.0) are shown.

plexes were determined as a function of pH as described previously (20). The pK_a values of the [^{13}C]dimethyl lysines were obtained by nonlinear regression fitting of the chemical shifts at different pH values to the Henderson-Hasselbalch equation with the Graph Pad Prism computer program (GraphPad Software, San Diego, CA). The sigmoidal equation is

$$Y = [U + W \times 10^{(X-X_c)}]/[10^{(X-X_c)} + 1]$$

where Y is the chemical shift, U is the lower limit of the shift, W is the upper limit, X is pH, and X_c is pK_a.

Analytical procedures

Protein concentrations were determined by the Lowry procedure (30), and phospholipid content was determined by phosphorus analysis (31). ^{14}C radioactivity was assessed by standard liquid scintillation procedures. Polyacrylamide gel electrophoresis (8–25% gradient) in the presence or absence of SDS was performed with a Pharmacia (Piscataway, NJ) Phast electrophoresis system to monitor the purity of the proteins or to determine the size of the DMPC complexes. Circular dichroism spectra were obtained on a Jasco (Easton, MD) J600 spectropolarimeter equipped with a temperature-controlling device and interfaced with a computer. The α-helical content of each preparation was derived from the molar ellipticity at 222 nm by established procedures (26, 32).

RESULTS

Previously, we used two-dimensional NMR spectra of [^{13}C]dimethyl lysines to study the microenvironments in 22-kDa apoE·DMPC complexes (20). The lysine resonances were poorly resolved when the protein is present in the lipid-free state in the four-helix bundle conformation. **Figure 1A**

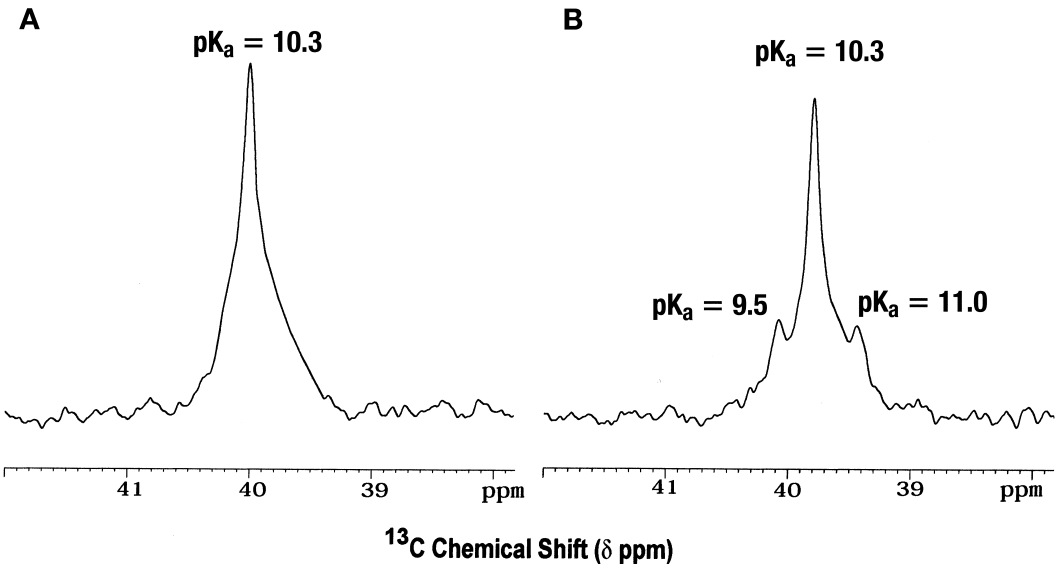

Fig. 2. Proton-decoupled ^{13}C NMR spectra of [ε-^{13}C]lysine 22-kDa apoE3 at 100.6 MHz. The degree of incorporation of [ε-^{13}C]lysine by expression in *E. coli* was 50%. A: Lipid-free 22-kDa apoE3 (1.9 mg/ml) was dissolved in borate-buffered D_2O. B: 22-kDa apoE3 (1.8 mg/ml) was dissolved as a 1:3.2 (w/w) complex with DMPC. The pK_a values were derived by measuring the chemical shifts in spectra obtained at different pH values. The spectra were obtained at 37°C, and 2,600 transients were accumulated with CPD decoupling and the MLEV sequence. Chemical shifts are given in parts per million with aqueous 1,4-dioxane (66.55) as external reference.

shows an NMR spectrum and the sequence-specific assignment of the eight [^{13}C]dimethyl lysine resonances apparent when the 22-kDa apoE3 is associated with DMPC. This enhanced resolution reflects the changes in lysine microenvironments induced by the opening of the four-helix bundle on interaction with DMPC. These changes are accompanied by an ~10^4-fold increase in the affinity of the 22-kDa apoE3 molecule for the LDLR. Using a fibroblast LDLR competitive binding assay (17), the concentrations of 22-kDa apoE3 required to reduce binding of ^{125}I-labeled LDL to the LDLR by 50% were 7,000 and 0.7 nM for the lipid-free protein and protein complexed to DMPC, respectively. Figure 1B shows a similar two-dimensional NMR spectrum for a 22-kDa apoE2·DMPC complex. The resonances from the eight [^{13}C]dimethyl lysine residues are again resolved. The resonance with a ^{13}C chemical shift (δ) of 41.0 ppm is from the N-terminal α-amino group; the lysine assignments were made by comparison with ^{13}C chemical shifts and pK_a values observed for 22-kDa apoE3·DMPC discs (20). As with apoE3 (20), the spectrum of lipid-free 22-kDa apoE2 was poorly resolved (data not shown), suggesting that apoE2 and apoE3 undergo similar conformational rearrangements on interaction with DMPC.

Several control experiments confirmed that dimethylation of the lysines in apoE does not perturb their titration characteristics. Dimethylation does not alter the lipid-binding properties of apoE (26). The δ of [ε-^{13}C]lysine reflects the titration of the ε-amino group (33). In our hands, the δ of [ε-^{13}C]lysine in solution increased from 39.1 to 40.3 ppm as the pH was raised from 8 to 12, and the pK_a was 10.5. **Figure 2A** shows the [ε-^{13}C]lysine resonance after incorporation into lipid-free 22-kDa apoE. A single broad resonance was apparent at δ = 40.1 ppm. When δ was measured as a function of pH, the pK_a was 10.3. This result agrees with the values obtained from two-dimensional NMR spectra of [^{13}C]dimethyl lysine 22-kDa apoE3 (20). There was no advantage in using two-dimensional spectra with the [ε-^{13}C]lysine apoE; the protons attached to the ^{13}C atom resonated as a triplet (because of coupling with protons on the adjacent methylene group), reducing resolution in the ^{1}H dimension. As with [^{13}C]dimethyl lysine 22-kDa apoE3 (20), the interaction with DMPC altered the pK_a of the lysines. Three resonances at δ = 39.4, 39.8, and 40.1 ppm were resolved in the spectrum of an [ε-^{13}C]lysine 22-kDa apoE·DMPC complex (Fig. 2B). Titration curves (**Fig. 3**) show that most lysines retained a pK_a of ~10.3, but subsets of lysines had pK_a values of 9.5 and 11.0, consistent with the low pK_a values of K143 and K146 (9.2–9.5) and the higher pK_a of K157 (11.1) previously obtained with [^{13}C]dimethyl lysine 22-kDa apoE3 (20). Overall, our results confirm that valid information about the microenvironments of lysine in apoE can be obtained by using ^{13}C-dimethylated protein (Figs. 2 and 3). This is consistent with the fact that dimethylation of lysines does not significantly perturb protein structure or lysine pK_a values (21).

NMR spectra were obtained at various pH values to generate titration curves (**Fig. 4A**). The pK_a values for K143, K146, and K157, which are located on helix 4 of 22-kDa apoE2 (15), were 9.4, 9.9, and 10.9, respectively. The pK_a

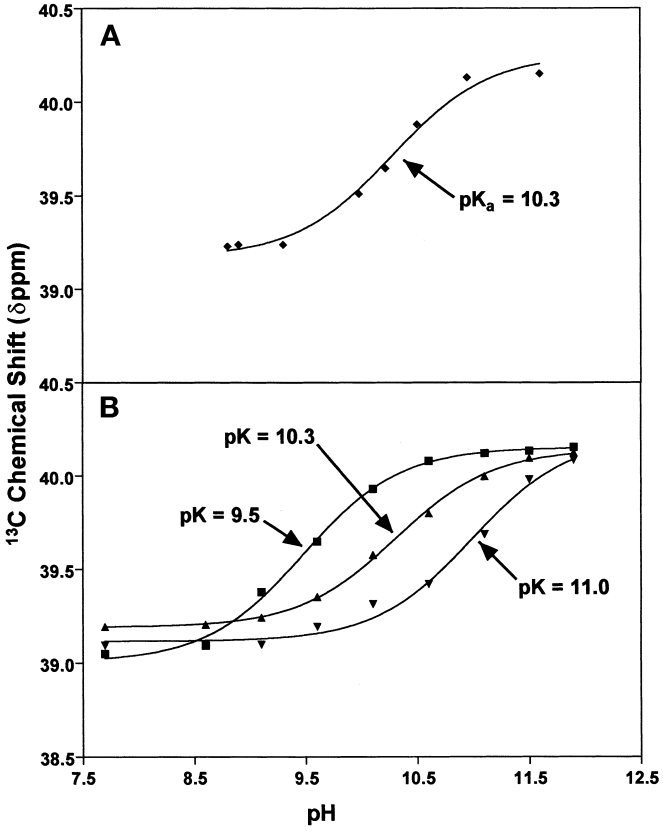

Fig. 3. ^{13}C NMR chemical shifts (ppm) as a function of pH for the [ε-^{13}C]lysine resonances of [ε-^{13}C]lysine 22-kDa apoE3. The chemical shifts were obtained from spectra of the type shown in Fig. 2. The pH titration curves and pK_a values for lysines were obtained by nonlinear regression fitting to the Henderson-Hasselbalch equation, as described in Experimental Methods. A: pH dependence of the [ε-^{13}C]lysine resonance from lipid-free [ε-^{13}C]lysine 22-kDa apoE3 dissolved in borate buffer (cf. Fig. 2A). B: pH dependence of the [ε-^{13}C]lysine resonances from an [ε-^{13}C]lysine 22-kDa apoE3·DMPC complex. The three resonances are shown in Fig. 2B at δ = 40.1 ppm (solid squares), 39.8 ppm (solid triangles), and 39.4 ppm (solid inverted triangles).

values for all the lysines in 22-kDa apoE2 and 22-kDa apoE4 are listed in **Table 1**, together with the values for 22-kDa apoE3 reported previously (20). Most lysine pK_a values were not affected uniformly by the polymorphism. In contrast, the pK_a values of K143 and K146 in apoE2, apoE3 and apoE4 differed significantly. Both lysines are in the LDLR-binding region, and their pK_a values reflect the functionality of the domain with respect to recognition by the receptor. When complexed with DMPC, full-length apoE3 and apoE4 and their 22-kDa fragments have the same affinity for the LDLR (4, 34). In contrast, the affinity of full-length apoE2 is ~1% that of apoE3, and the affinity of the 22-kDa fragment is ~10% (4). This difference reflects the influence of the C-terminal domain on receptor-binding activity (13). Conversion of cysteines in the apoE2 22-kDa fragment to positively charged lysine analogs by treatment with cysteamine increases the binding affinity to near normal levels (4). Consistent with the requirement for an appropriate microenvironment in the LDLR-

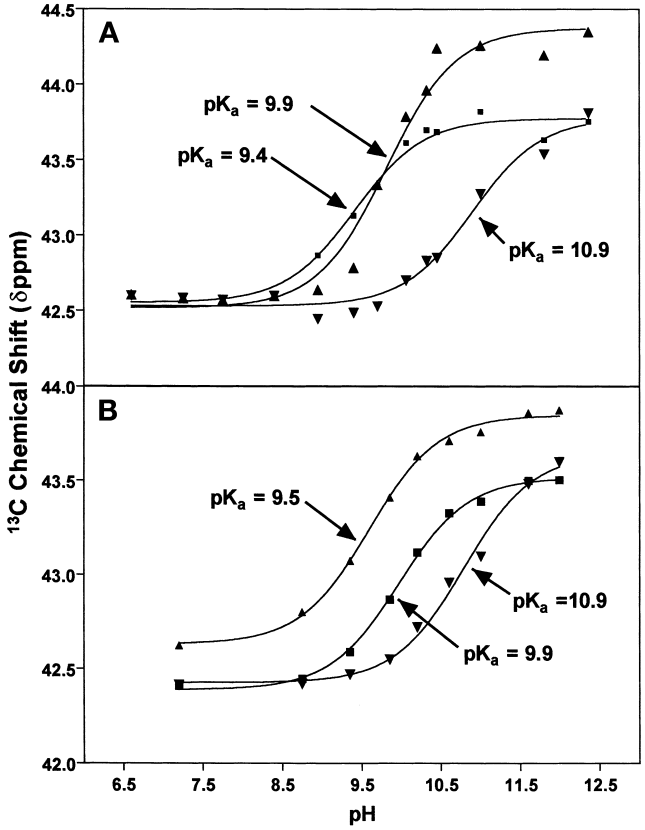

Fig. 4. ^{13}C NMR chemical shifts (ppm) as a function of pH for the resonances from selected [^{13}C]dimethyl lysine residues of 22-kDa apoE2·DMPC discoidal complexes. The chemical shifts were obtained from NMR spectra of the type shown in Fig. 1. The pK$_a$ values were obtained as described in Fig. 3. A: 22-kDa apoE2·DMPC. B: Cysteamine-modified 22-kDa apoE2·DMPC. K143 (solid squares), K146 (solid triangles), K157 (solid inverted triangles).

binding region of apoE, treatment of apoE2 with cysteamine affected the pK$_a$ values of K143 and K146 (Fig. 4B and Table 1). This chemical modification did not alter the pK$_a$ of K157, which is also located in helix 4.

Because binding of apoE to the LDLR is influenced by the degree of exposure of the polar face of helix 4 to the aqueous phase (20), ferricyanide shift reagent experiments were performed to assess the effects of apoE polymorphism on the relative exposure of K143 and K146 to the aqueous phase (**Table 2**). In all cases, ferricyanide shifted the resonances of K143 and K146 downfield more than the other lysine resonances. Thus, the cysteine/arginine interchanges at positions 112 and 158 that differentiate the apoE isoforms did not significantly affect the exposure of any of the lysines to the aqueous phase.

DISCUSSION

The greater affinity of lipid-bound apoE3 for the LDLR, compared with lipid-free apoE3, is a consequence of reorganization of the α-helical domains. This reorganization involves opening of the N-terminal four-helix bundle

TABLE 1. Lysine pK$_a$ values in apoE isoforms

Lysine Residue	pK$_a$[a]			
	ApoE2	Cysteamine-ApoE2[b]	ApoE3	ApoE4
	pH units			
1	10.2	10.1	10.5	10.1
69	10.1	10.1	10.4	10.1
72	10.0	10.0	10.0	10.0
75	10.0	10.0	10.1	10.1
95	10.2	10.2	10.1	10.1
143	9.4	9.9	9.5	9.9
146	9.9	9.5	9.2	9.4
157	10.9	10.9	11.1	10.9

[a] The pK$_a$ values (±0.1 pH unit) were derived from the pH dependence of ^{13}C chemical shifts measured in two-dimensional NMR spectra of 22-kDa apoE·DMPC discoidal complexes. These complexes were similar for the three apoE isoforms; the lipid:protein stoichiometry was 3.2:1 (w/w), the hydrodynamic diameter was ~16 nm, and the α-helical content of the apoE was 65–70% (20).

[b] The cysteine residues in the 22-kDa apoE2·DMPC disc were converted to positively charged lysine analogs with cysteamine, as described in Experimental Methods.

structure (18, 19), which leads to changes in interhelical interactions. Activation of the LDLR-binding region (residues 136–150) involves two changes in the microenvironment. First, removal of interhelical salt bridges increases the positive electrostatic potential. Second, limited penetration of the amphipathic α-helix into the nonpolar lipid milieu increases the relative exposure to the aqueous phase (20). The same effects confer full LDLR-binding affinity on apoE4 complexed to lipid but not on apoE2 (4). In the current studies, we directly demonstrated that the microenvironments of apoE2 and apoE3 differ in the LDLR-binding region when complexed with lipid and that the positive charge of the receptor-binding region in apoE2 is significantly reduced.

Comparison of the pK$_a$ values of lysines in the four-helix bundle (Table 1) showed that the environments in helices 2 and 3 are similar for the three isoforms. The pK$_a$ values of K72 and K75 in helix 2 and of K95 in helix 3 were

TABLE 2. Potassium ferricyanide-induced changes in NMR spectra of the 22-kDa apoE isoforms in DMPC discs

^{13}C Resonance	Relative Downfield Shift[a]		
	ApoE2	ApoE3	ApoE4
DMPC-N(CH$_3$)$_3$	1.00	1.00	1.00
α-N terminal	0.22	0.15	0.24
Lys-1	0.72	0.60	0.65
Lys-69	0.22	0.15	0.12
Lys-72	0.67	0.55	0.59
Lys-75	0.11	0.15	0.12
Lys-95	0.56	0.60	0.59
Lys-143	1.11	0.95	0.95
Lys-146	1.56	1.25	1.18
Lys-157	0.56	0.55	0.59

[a] The values are normalized to the changes in δ for the DMPC-N(CH$_3$)$_3$ peak, which resonated at 54.18 ± 0.01 ppm in the absence of shift reagent. K$_3$Fe(CN)$_6$ added at a 0.5 molar ratio relative to the DMPC induced downfield shifts of 0.18, 0.20, and 0.17 ppm, respectively, in the DMPC-N(CH$_3$)$_3$ resonance in apoE·DMPC discs. The spectra were obtained at pH 10.4 ± 0.2.

largely unaffected by the cysteine/arginine interchanges at positions 112 and 158. Somewhat surprisingly, the pK_a value of K157 in helix 4 was the same in all three isoforms, despite the C158R mutation that distinguishes apoE2 from apoE3 and apoE4 (Table 1). The introduction of positive charges at C112 and C158 in apoE2 by cysteamine modification did not alter the pK_a of any lysine outside the LDLR-binding region on helix 4.

The differences in the pK_a values of K143 and K146 in lipid-complexed apoE isoforms are consistent with the notion that the mutations at positions 112 and 158 directly influence the LDLR-binding region. The changes in lysine in pK_a values in this region reflect variations in the positive electrostatic potential in the microenvironment (20); this potential influences the affinity for the LDLR. Despite differences in the basicity of the LDLR-binding region in the apoE isoforms, the polar face of helix 4 seems to be similarly exposed to the aqueous phase in all three isoforms, as suggested by the ferricyanide shift reagent experiments (Table 2). Changes in δ for K143 and K146 were similar for all three isoforms and for cysteamine-treated 22-kDa apoE2. Thus, the differences in the LDLR-binding affinities of apoE2 and apoE3 do not reflect differences in penetration of the amphipathic α-helix containing residues 136–150 into the nonpolar lipid environment.

Effect of the R158C mutation

The 22-kDa apoE3·DMPC complex binds with maximal affinity to the LDLR (34), and the pK_a values of K143 and K146 are 9.5 and 9.2, respectively (Table 1). These values are unusually low because the increased positive electrostatic potential in the LDLR-binding region reduces the affinity of the ε-amino groups for protons (20). The local positive charge appears to be greater near the K146 side chain because K146 has a lower pK_a than K143. The R158C mutation in apoE2 has little effect on the pK_a of K143 but increases the pK_a of K146 by 0.7 pH unit to 9.9. This increase reflects a loss of basicity in the immediate environment of the K146 side chain and is associated with reduced LDLR-binding affinity (1% of apoE3) (4). The change in basicity around K146 is consistent with X-ray crystallography of lipid-free 22-kDa fragments of apoE2 and apoE3 (12, 14, 15). In apoE3, there is a salt bridge between D154 and R158; because of the R158C substitution in apoE2, this salt bridge is replaced with a D154–R150 salt bridge (12, 15). This new interaction reduces the net positive charge on the R150 side chain and shifts it out of the receptor-binding region. The positions of these residues along the polar face of helix 4 in apoE2 and apoE3 are shown in **Fig. 5**.

NMR measurements of the pK_a values for K143 and K146 in 22-kDa apoE·DMPC complexes strongly suggest that the intrahelical ionic interactions in helix 4 are similar in the lipid-free and lipidated 22-kDa apoE molecules. The partial neutralization of the R150 positive charge in apoE2 by participation in a salt bridge with D154 (15) would be expected to reduce the net positive electrostatic potential experienced by K146, located one turn along the α-helix from R150 (Fig. 5). This is reflected by an increase in the pK_a from 9.2 in apoE3 to 9.9 in apoE2 (Table 1). Restoration of a positive charge at position 158 by treatment of apoE2 with cysteamine decreased the pK_a of K146 to 9.5. This reflects partial restoration of the basicity in this microenvironment because D154 interacts not only

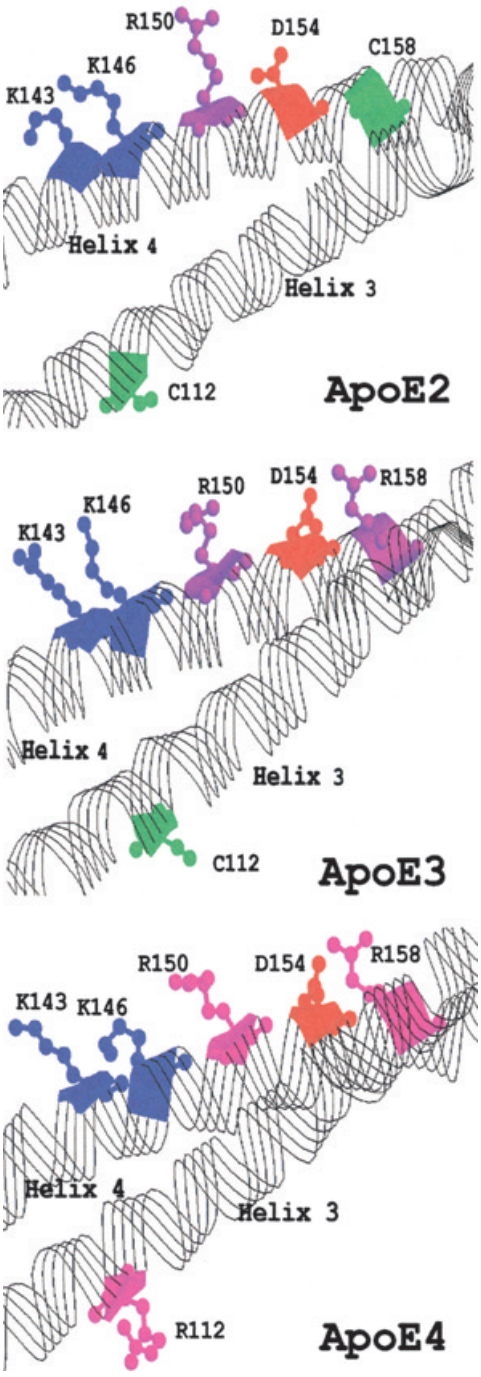

Fig. 5. Organization of selected residues on the amphipathic α-helices 3 and 4 in lipid-free 22-kDa apoE isoforms. The crystal structure coordinates are from previous publications (14–16) and the pictures are drawn with RasMol (38). The α-helix backbones are shown as strands, and the amino acid side chains are drawn as balls and sticks. The juxtaposition of the D154 and R158 side chains in apoE3 and apoE4 is shown in the bottom two panels. The juxtaposition of the D154 and R150 side chains in apoE2 is shown in the top panel.

with R150 but also with the positive charge at position 158 created by the cysteamine modification.

In lipid-associated 22-kDa fragments of apoE2 and apoE3, K143 has the same pK_a value (~9.5) (Table 1). This indicates that the C158R mutation does not affect basicity in the microenvironment of the K143 side chain (Fig. 5). Although the pK_a of K143 in apoE4 is 9.9, this isoform binds as well as apoE3 to the LDLR, suggesting that the magnitude of the positive electrostatic potential around K143 is less important for receptor binding than that around K146. This suggestion is consistent with the idea that ligand recognition by repeat modules of the LDLR is mediated by electrostatic complementarity of conserved patches of negative electrostatic potential on the receptor (35) and the positive charge of apoE. The net positive charges of the lysine side chains at positions 143 and 146 are both important for LDLR interaction because replacement of either lysine with a neutral amino acid reduces binding to about 25–30% of the apoE3 value (36).

Role of the C112R mutation

Although the presence of a positive charge at position 112 in apoE4 does not alter LDLR-binding affinity (4), it increased the pK_a of K143 by ~0.4 pH unit (Table 1). It is not obvious from examination of the four-helix bundle structure formed by 22-kDa apoE3 and apoE4 (Fig. 5) why this would occur. In the lipid-free four-helix bundle structure, R112 is ~20 Å from K143 on the opposite side of helix 3, so the residues are too far apart to interact. However, the pK_a data show that there is an interaction when the four-helix bundle is open and the protein is associated with DMPC in a discoidal complex. These two residues are located at similar positions along helices 3 and 4 but protrude away from each another in the bundle. If interaction with lipid induced rotation in these helices, bringing R112 and K143 into closer proximity, then the observed change in pK_a values of K143 in apoE4 would be explained. It is plausible that helix 3 in apoE·DMPC complexes is oriented differently in apoE3 and apoE4. In apoE3, C112 is located on the nonpolar face of the amphipathic α-helix 3 (37); in apoE4, the introduction of R112 disrupts the nonpolar face, reducing its angle from 180° to 120° and likely inducing a rotation of the α-helix with respect to the plane of the lipid-water interface. These suggested effects of the R112–K143 interaction are based on the assumption that intramolecular effects predominate. However, intermolecular interactions between helices 3 and 4 could give rise to similar effects. The interaction apparently involves more than simple juxtaposition of the positively charged R112 and K143 side chains. If that were the case, the pK_a of K143 would be expected to decrease rather than increase.

Summary and conclusions

For optimal high-affinity binding of apoE to the LDLR, the microenvironment in the LDLR-binding region must have the appropriate distribution of positive electrostatic potential and degree of exposure to the aqueous phase (20). Interaction with lipid alters helix-helix interactions in the four-helix bundle structure, causing the LDLR-binding region spanning residues 136–150 on helix 4 to assume a high-affinity binding conformation. Comparison of the pK_a values of K143 and K146 in 22-kDa apoE2·DMPC and apoE3·DMPC complexes reveals that the R158C mutation in apoE2 alters the microenvironment in the LDLR-binding region; this is associated with the decrease in receptor-binding affinity. The C112R substitution in apoE4 also affects the microenvironment in the receptor-binding region because the pK_a of K143 is increased. Because this change has no effect on receptor binding, it seems that the C-terminal portion of this region plays a more critical role than the N-terminal portion in the interaction with the LDLR. These insights into the molecular features required for high affinity binding provide a basis for designing ways to enhance the binding of apoE to the LDLR.

We thank Faye Baldwin and Padmaja Dhanasekaran for expert technical assistance, and Gary Howard and Stephen Ordway for excellent editorial assistance. Mass spectra were provided by the UCSF Mass Spectrometry Facility (A. L. Burlingame, Director) supported by the Biomedical Research Technology Program of the National Center for Research Resources, NIH NCRR BRTP RR01614. This work was supported by NIH grants HL56083 and HL41633.

Manuscript received 12 December 2000 and in revised form 22 February 2001.

REFERENCES

1. Mahley, R. W., and S-Z. Ji. 1999. Remnant lipoprotein metabolism: key pathways involving cell-surface heparan sulfate proteoglycans and apolipoprotein E. *J. Lipid. Res.* **40:** 1–16.
2. Mahley, R. W., and Y. Huang. 1999. Apolipoprotein E: from atherosclerosis to Alzheimer's disease and beyond. *Curr. Opin. Lipidol.* **10:** 207–217.
3. Weisgraber, K. H. 1994. Apolipoprotein E: structure-function relationships. *Adv. Protein Chem.* **45:** 249–302.
4. Weisgraber, K. H., T. L. Innerarity, and R. W. Mahley. 1982. Abnormal lipoprotein receptor-binding activity of the human E apoprotein due to cysteine-arginine interchange at a single site. *J. Biol. Chem.* **257:** 2518–2521.
5. Mahley, R. W., Y. Huang, and S. C. Rall, Jr. 1999. Pathogenesis of type III hyperlipoproteinemia (dysbetalipoproteinemia): questions, quandaries, and paradoxes. *J. Lipid Res.* **40:** 1933–1949.
6. Utermann, G., A. Hardewig, and F. Zimmer. 1984. Apolipoprotein E phenotypes in patients with myocardial infarction. *Hum. Genet.* **65:** 237–241.
7. Luc, G., J-M. Bard, D. Arveiler, A. Evans, J-P. Cambou, A. Bingham, P. Amouyel, P. Schaffer, J-B. Ruidavets, F. Cambien, J-C. Fruchart, and P. Ducimetiere. 1984. Impact of apolipoprotein E polymorphism on lipoproteins and risk of myocardial infarction. *Arterioscler. Thromb.* **14:** 1412–1419.
8. Eichner, J. E., L. H. Kuller, T. J. Orchard, G. A. Grandits, L. M. McCallum, R. E. Ferrell, and J. D. Neaton. 1993. Relation of apolipoprotein E phenotype to myocardial infarction and mortality from coronary artery disease. *Am. J. Cardiol.* **71:** 160–165.
9. Weisgraber, K. H. 1990. Apolipoprotein E distribution among human plasma lipoproteins: role of the cysteine-arginine interchange at residue 112. *J. Lipid Res.* **31:** 1503–1511.
10. Weisgraber, K. H., and R. W. Mahley. 1996. Human apolipoprotein E: the Alzheimer's disease connection. *FASEB J.* **10:** 1485–1494.
11. Mahley, R. W. 1988. Apolipoprotein E: cholesterol transport protein with expanding role in cell biology. *Science.* **240:** 622–630.
12. Dong, L-M., S. Parkin, S. D. Trakhanov, B. Rupp, T. Simmons, K. S. Arnold, Y. M. Newhouse, T. L. Innerarity, and K. H. Weisgraber. 1996. Novel mechanism for defective receptor binding of apolipo-

protein E2 in type III hyperlipoproteinemia. *Nat. Struct. Biol.* **3:** 718–722.
13. Dong, L. M., T. L. Innerarity, K. S. Arnold, Y. M. Newhouse, and K. H. Weisgraber. 1998. The carboxyl terminus in apolipoprotein E2 and the seven amino acid repeat in apolipoprotein E-Leiden: role in receptor-binding activity. *J. Lipid Res.* **39:** 1173–1180.
14. Wilson, C., M. R. Wardell, K. H. Weisgraber, R. W. Mahley, and D. A. Agard. 1991. Three-dimensional structure of the LDL receptor-binding domain of human apolipoprotein E. *Science.* **252:** 1817–1822.
15. Wilson, C., T. Mau, K. H. Weisgraber, M. R. Wardell, R. W. Mahley, and D. A. Agard. 1994. Salt bridge relay triggers defective LDL receptor binding by a mutant apolipoprotein. *Structure.* **2:** 713–718.
16. Dong, L-M., C. Wilson, M. R. Wardell, T. Simmons, R. W. Mahley, K. H. Weisgraber, and D. A. Agard. 1994. Human apolipoprotein E. Role of arginine 61 in mediating the lipoprotein preferences of the E3 and E4 isoforms. *J. Biol. Chem.* **269:** 22358–22365.
17. Innerarity, T. L., R. E. Pitas, and R. W. Mahley. 1979. Binding of arginine-rich (E) apoprotein after recombination with phospholipid vesicles to the low density lipoprotein receptors of fibroblasts. *J. Biol. Chem.* **254:** 4186–4190.
18. Fisher, C. A., and R. O. Ryan. 1999. Lipid binding-induced conformational changes in the N-terminal domain of human apolipoprotein E. *J. Lipid Res.* **40:** 93–99.
19. Lu, B., J. A. Morrow, and K. H. Weisgraber. 2000. Conformational reorganization of the four-helix bundle of human apolipoprotein E in binding to phospholipid. *J. Biol. Chem.* **275:** 20775–20781.
20. Lund-Katz, S., M. Zaiou, S. Wehrli, P. Dhanasekaran, F. Baldwin, K. H. Weisgraber, and M. C. Phillips. 2000. Effects of lipid interaction on the lysine microenvironments in apolipoprotein E. *J. Biol. Chem.* **275:** 34459–34464.
21. Jentoft, N., and D. G. Dearborn. 1983. Protein labeling by reductive alkylation. *Methods Enzymol.* **91:** 570–579.
22. Morrow, J. A., K. S. Arnold, and K. H. Weisgraber. 1999. Functional characterization of apolipoprotein E isoforms overexpressed in *Escherichia coli*. *Protein Expr. Purif.* **16:** 224–230.
23. Segelke, B. W., M. Forstner, M. Knapp, S. Trakhanov, S. Parkin, Y. M. Newhouse, H. D. Bellamy, K. H. Weisgraber, and B. Rupp. 2000. Conformational flexibility in the apolipoprotein E amino-terminal domain structure determined from three new crystal forms: implications for lipid binding. *Protein Sci.* **9:** 886–897.
24. LeMaster, D. M., and F. M. Richards. 1985. ^{1}H-^{15}N heteronuclear NMR studies of *Escherichia coli* thioredoxin in samples isotopically labeled by residue type. *Biochemistry.* **24:** 7263–7268.
25. Scapin, G. J., C. Sacchettini, A. Dessen, M. Bhatia, and C. Grubmeyer. 1993. Primary structure and crystallization of orotate phosphoribosyltransferase from *Salmonella typhimurium*. *J. Mol. Biol.* **230:** 1304–1308.
26. Lund-Katz, S., K. H. Weisgraber, R. W. Mahley, and M. C. Phillips. 1993. Conformation of apolipoprotein E in lipoproteins. *J. Biol. Chem.* **268:** 23008–23015.
27. Innerarity, T. L., K. H. Weisgraber, K. S. Arnold, S. C. Rall, Jr., and R. W. Mahley. 1984. Normalization of receptor binding of apolipoprotein E2. Evidence for modulation of the binding site conformation. *J. Biol. Chem.* **259:** 7261–7267.
28. Marion, D., and A. H. Wyllie. 1983. Application of phase sensitive two-dimensional correlated spectroscopy (COSY) for measurements of ^{1}H-^{1}H spin-spin coupling constants in proteins. *Biochem. Biophys. Res. Commun.* **113:** 967–974.
29. Lund-Katz, S., J. A. Ibdah, J. Y. Letizia, M. T. Thomas, and M. C. Phillips. 1988. A ^{13}C NMR characterization of lysine residues in apolipoprotein B and their role in binding to the low density lipoprotein receptor. *J. Biol. Chem.* **263:** 13831–13838.
30. Lowry, O. H., N. J. Rosebrough, A. L. Farr, and R. J. Randall. 1951. Protein measurement with the Folin phenol reagent. *J. Biol. Chem.* **193:** 265–275.
31. Sokoloff, L., and G. H. Rothblat. 1974. Sterol to phospholipid molar ratios of L-cells with qualitative and quantitative variations of cellular sterol. *Proc. Soc. Exp. Biol. Med.* **146:** 1166–1172.
32. Sparks, D. L., M. C. Phillips, and S. Lund-Katz. 1992. The conformation of apolipoprotein A-I in discoidal and spherical recombinant high density lipoprotein particles. *J. Biol. Chem.* **267:** 25830–25838.
33. Christl, M., and J. D. Roberts. 1972. Nuclear magnetic resonance spectroscopy. Carbon-13 chemical shifts of small peptides as a function of pH. *J. Am. Chem. Soc.* **94:** 4565–4573.
34. Innerarity, T. L., E. J. Friedlander, Jr., S. C. Rall, K. H. Weisgraber, and R. W. Mahley. 1983. The receptor-binding domain of human apolipoprotein E. Binding of apolipoprotein E fragments. *J. Biol. Chem.* **258:** 12341–12347.
35. North, C. L., and S. Blacklow. 2000. Solution structure of the sixth LDL-A module of the LDL receptor. *Biochemistry.* **39:** 2564–2571.
36. Zaiou, M., K. S. Arnold, Y. M. Newhouse, T. L. Innerarity, K. H. Weisgraber, M. L. Segall, M. C. Phillips, and S. Lund-Katz. 2000. Apolipoprotein E-low density lipoprotein receptor interaction: influences of basic residue and amphipathic alpha-helix organization in the ligand. *J. Lipid Res.* **41:** 1087–1095.
37. Anantharamaiah, G. M., M. K. Jones, and J. P. Segrest. 1993. An atlas of the amphipathic helical domains of human exchangeable plasma apolipoproteins. *In* The Amphipathic Helix. R. M. Epand, editor. CRC Press, Boca Raton, FL. 109–142.
38. Sayle, R., and E. J. Milner-White. 1995. RasMol: biomolecular graphics for all. *Trends Biochem. Sci.* **20:** 374.